Available online at www.sciencedirect.com
SCIENCE DIRECT®
Bioorganic & Medicinal Chemistry Letters 15 (2005) 2409–2413
Bioorganic & Medicinal Chemistry Letters

Design and synthesis of potent pyridazine inhibitors of p38 MAP kinase

Nuria Tamayo,[a,*] Lillian Liao,[a] Martin Goldberg,[a] David Powers,[a] Yan-Yan Tudor,[a] Violeta Yu,[a] Lu Min Wong,[b] Bradley Henkle,[b] Scot Middleton,[b] Rashid Syed,[a] Timothy Harvey,[a] Graham Jang,[c] Randall Hungate[a] and Celia Dominguez[a,*]

[a]*Chemistry Research and Discovery, Amgen, Inc., One Amgen Center Drive, Thousand Oaks, CA 91320, USA*
[b]*Inflammation, Amgen, Inc., One Amgen Center Drive, Thousand Oaks, CA 91320, USA*
[c]*Pharmacokinetics and Drug Metabolism, Amgen, Inc., One Amgen Center Drive, Thousand Oaks, CA 91320, USA*

Received 11 January 2005; revised 2 February 2005; accepted 3 February 2005
Available online 22 March 2005

Abstract—Novel potent trisubstituted pyridazine inhibitors of p38 MAP (mitogen activated protein) kinase are described that have activity in both cell-based assays of cytokine release and animal models of rheumatoid arthritis. They demonstrated potent inhibition of LPS-induced TNF-α production in mice and exhibited good efficacy in the rat collagen induced arthritis model.

1. Introduction

Inhibitors of p38 mitogen activated protein (MAP) kinase inhibit the production of proinflammatory cytokines, for example, tumor necrosis factor-α (TNF-α) and interleukin-1β (IL-1β), whose accumulation initiates a cascade of events leading to inflammation and tissue destruction in diseases such as rheumatoid arthritis (RA),[1] Crohn's disease,[2] inflammatory bowel syndrome, and psoriasis. The inhibition of TNF-α and IL-1β presents a useful therapeutic strategy to suppress the inflammation and prevent joint damage caused by RA, as shown by the newer biologic therapies for RA (etanercept, infliximab, adalimumab, and anakinra) that target these cytokines. p38 MAP kinase is a member of a family of serine–threonine kinases that are activated by dual phosphorylation of a TGY motif.[3] This phosphorylation is carried out by dual specificity kinases (MKK3 and MKK6[4]) in response to extracellular stimuli such as osmotic shock, endotoxins (lipopolysaccharide, LPS), UV light or cytokines.[5]

Therefore, pharmacological inhibition of p38 kinase is a potential therapy for inflammatory conditions due to excessive cytokine production.

Keywords: p38 Kinase inhibitors; Pyridazines.
* Corresponding authors. Tel.: +1 805 447 8814; fax: +1 805 480 1337; e-mail: ntamayo@amgen.com

0960-894X/$ - see front matter © 2005 Elsevier Ltd. All rights reserved.
doi:10.1016/j.bmcl.2005.02.010

2. Chemistry

3,4,6-Trisubstituted pyridazines were prepared by reaction of hydrazine with either a 1,4-diketone or a 1,4-diketoester.[6,7] Aromatization of the cyclized adducts followed by functional group modifications provided the target analogues.

The preparation of 6-substituted carbon analogues is shown in Scheme 1. Ketones **1** and **2** were prepared by reaction of the anion derived from either 2-fluoro-4-methylpyridine (**3**) or 4-methyl-2-(methylthio)pyrimidine[8] (**4**) with the Weinreb amide of 3-trifluoromethylbenzoic acid (**5**). Alkylation of the enolates of **1** and **2** with 4-(2-chloroacetyl)-piperidine-1-carboxylic acid benzyl ester[9] led to the 1,4-diketones **6** and **7**, respectively. The cyclization to form the 3,4-dihydropyridazines was carried out by heating the 1,4-diketones with hydrazine in *t*-butanol under reflux followed by evaporation of the solvent and heating at 180 °C under high vacuum. Aromatization by oxidation using DDQ in toluene provided the pyridazines **8** and **9**. The pyridazine **8** was converted to the analogue **10** by nucleophilic displacement of the fluoride in neat (*S*)-α-methylbenzylamine followed by hydrogenolysis of the protecting group. Sulfide **9** was oxidized to the sulfone **11** by heating under reflux with 30% hydrogen peroxide and sodium tungstate in methanol.[10] Nucleophilic displacement of the sulfone with different amines led to **12**, **13**,

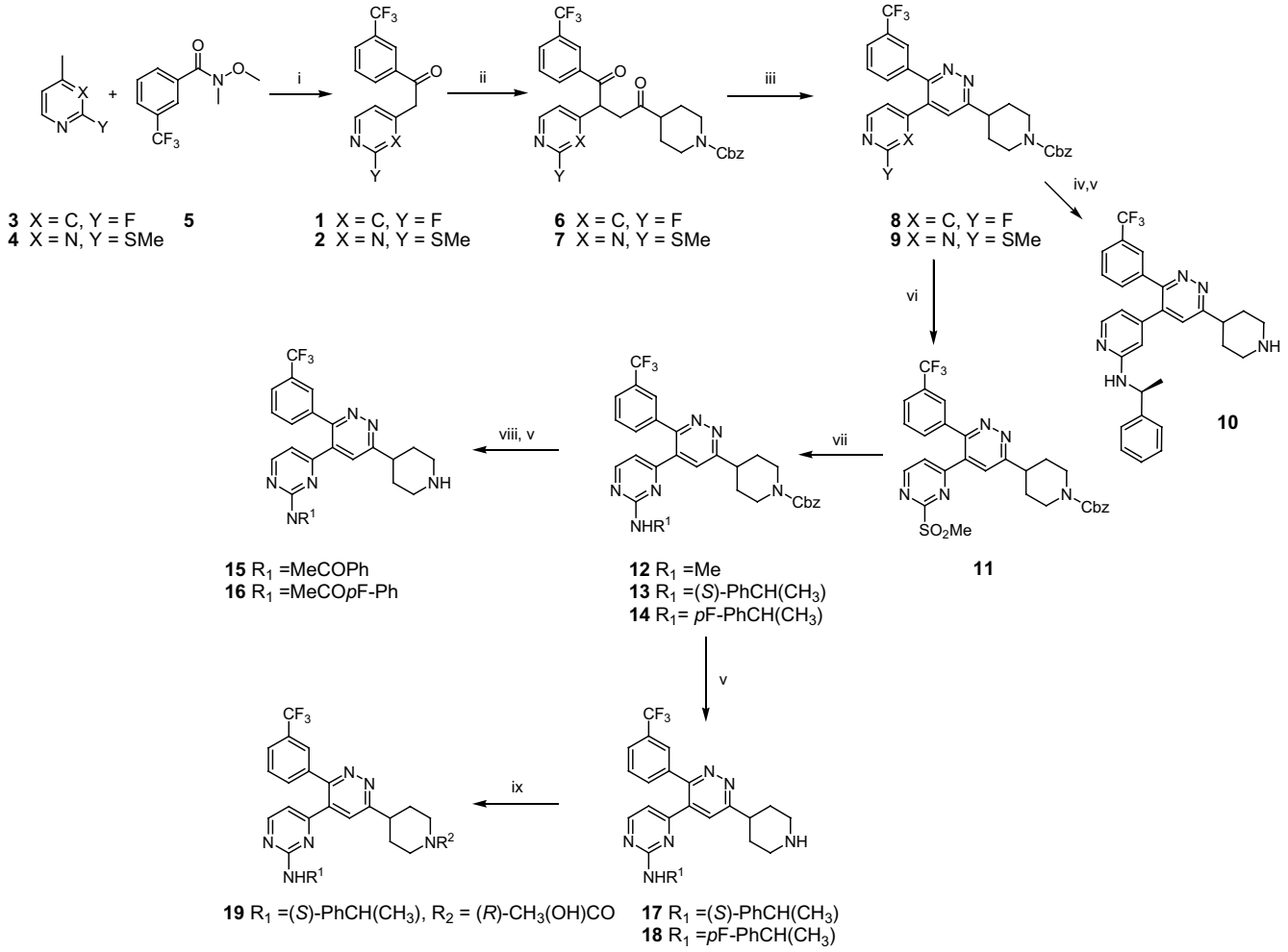

Scheme 1. Synthesis of piperidine-pyridazines. Reagents and conditions: (i) LDA, THF, −78 °C, 60–64%; (ii) 60% NaH, DMSO, rt, 0.5 h then 4-(2-chloroacetyl)-piperidine-1-carboxylic acid benzyl ester, rt, 18 h, 26–28%; (iii) (a) N_2H_4, *t*-BuOH, reflux, 0.5 h, then neat heated at 180 °C under high vacuum; (b) DDQ, toluene, rt, 18 h, 32–75%; (iv) (*S*)-α-methylbenzylamine, 125 °C, 3 h, 70%; (v) Pd/C, H_2, rt, 18 h, 31–87%; (vi) 30% H_2O_2, $Na_2WO_4{\cdot}2H_2O$, MeOH, reflux, 18 h, 90%; (vii) R^1NH_2 neat 125 °C, 57–70%; (viii) ArCOCl, Et_3N, DCM, rt, 88–95%; (ix) EDC, HOBt, (*R*)-lactic acid, 93%.

and **14**. Acylation of **12** with benzoyl chloride or *p*-fluorobenzoyl chloride followed by deprotection of the Cbz group afforded the analogues **15** and **16**. Hydrogenolysis of **13** and **14** gave pyridazines **17** and **18**. Compound **17** was further acylated with lactic acid to give **19**.

Synthesis of the 6-amino substituted analogues is illustrated in Scheme 2. Ketones **24** and **25** were synthesized by condensing the anion derived from 2-methylpyrimidine (**20**) or 4-picoline (**21**) with the Weinreb amides **22** and **23**, respectively. Alkylation of the enolatates derived from the ketones **24** and **25** with ethyl bromoacetate led to the ketoesters **26** and **27**, respectively. Cyclization with hydrazine in *t*-butanol, followed by oxidation with bromine in acetic acid afforded hydroxypyridazines **28** and **29**. Treatment of **28** and **29** with phosphorous trichloride gave the chloropyridazines **30** and **31**, respectively. The target analogues **32**–**41** were then prepared by treatment of the corresponding chloropyridazine with primary or secondary amines.

3. Biological results and discussion

Many small molecular inhibitors of p38 MAPK present a similar structural motif containing a vicinal pyridin-4-yl/phenyl group attached to a central heterocyclic core.[11] Crystallographic studies have shown that these types of p38 inhibitors bind to the ATP binding pocket of the enzyme.[12] The pyridyl nitrogen forms a key hydrogen bond interaction with the main chain NH of Met109 and the aromatic group occupies the lipophilic pocket, which includes residues Ala51, Lys53, Leu75, Ile84, Leu86, Leu104, and Thr106. However, many of these inhibitors, although very potent in vitro and in vivo, have shown significant hepatotoxicity in part due to their inhibition of cytochrome p450's.[11] Recently, several groups have disclosed new analogues that incorporated an α-substituted aminopyridine or aminopyrimidine moiety in place of an unsubstituted pyridine or pyrimidine with decreased p450 inhibition.[13] Our approach was to design and prepare compounds that incorporated some of these features using a

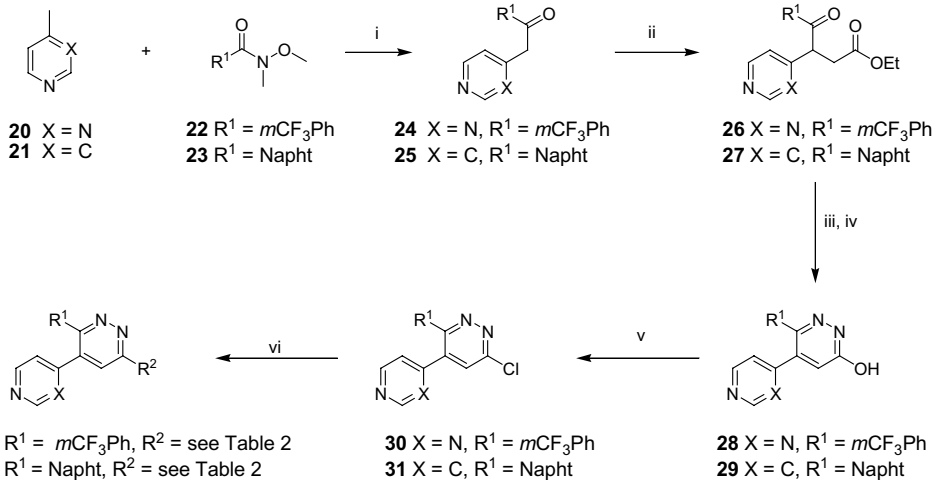

Scheme 2. Synthesis of aminopyridazines. Reagents and conditions: (i) LDA, THF, −78 °C, 69–72%; (ii) 60% NaH, DMSO, 0 °C, 45 min then ethyl bromoacetate, rt, 18 h, 20%; (iii) N_2H_4, *t*-BuOH, reflux, 0.5 h, then neat 180 °C under high vacuum, quant; (iv) Br_2, AcOH, 95 °C, 2 h, 51–63%; (v) $POCl_3$, Et_3BzNCl, iPr_2EtN, 100 °C, 2 h, 58–76%; (vi) R^2NH, K_2CO_3, NMP, 100 °C, 18 h, 10–35%.

pyridazine as a central scaffold.[6] In the first series of analogues (**10** and **17**) we confirmed what was previously reported for the imidazole series.[14] Both compounds are very potent in the binding and cellular assays[15,16] (see Table 1). However, their pharmacokinetic properties are distinct. Using human liver microsomes we determined that the pyrimidine analogue **17** is more metabolically stable than **10** (125 vs 750 μL/min/mg), this could be in part due to the reduced basicity of the pyrimidine nitrogen compared to the pyridine, decreasing its tendency to oxidation. We also tried to improve potency by introducing an α-hydroxyamide on the piperidine ring (**19**), this analogue although very potent is rapidly cleared. Using molecular modeling based on the co-crystal structures of closely related analogues (unpublished data), we determined the mode of binding of this type of trisubstituted pyridazines. As expected, the aryl substituent (mCF_3-phenyl and napthyl) of the pyridazine core fills the previously mentioned hydrophobic pocket (Ala51, Lys53, Leu75, Ile84, Leu86, Leu104, and Thr106) and the pyridyl/pyrimydyl nitrogen (*p*-position) forms a key hydrogen bond interaction with the NH of Met109. The phenyl group on the pyridine/pyrimidine substituent occupies a second hydrophobic pocket around the linker residues (Met109, Gly110, Ala111, and Asp112) and residue Leu167. To utilize these important hydrophobic interactions we designed a second series of compounds having a lipophilic amine linked to the 6-position on the central core (Table 2). With the assistance of co-crystal structures[17] and molecular modeling we postulated that these two types of compounds utilize very similar protein residue interactions (see Fig. 1). Although we were able to get a new key interaction between the amino group on the side chain and the backbone of Ser154 (see Fig. 2)[18] the new series is in general less potent than the original carbon analogues (cf. **17** and **32**). The pyridine analogues are 10-fold more potent than the pyrimidine (cf. **32** and **34**). Introduction of substituent at the aromatic ring on **34** did not affect potency (**35**). Secondary or tertiary amines were well tolerated at the 6-position (**34** and **39**) however, when the nitrogen at the 6-position is tertiary, the compounds are less selective against JNK3. Alkylation of the side chain nitrogen only reduces the potency slightly (**34** vs

Table 1. SAR of piperidyl/pyridazines

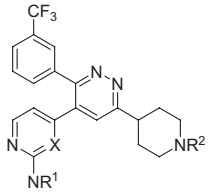

Compd	X	R^1	R^2	p38 (K_i, nM)	JNK3 (K_i, nM)	THP–TNF (IC_{50}, nM)
10	C	(*S*)-PhCH(CH_3)	H	2.1 ± 0.3	2970 ± 31	21.5 ± 0.6
15	N	MeCOPh	H	709 ± 15	>10,000	1286 ± 153
16	N	MeCO-*p*FPh	H	1772 ± 82	>10,000	1245 ± 54
17	N	(*S*)-PhCH(CH_3)	H	1.6 ± 0.2	1584 ± 147	5.3 ± 0.1
18	N	*p*F-PhCH(CH_3)	H	10.2 ± 0.5	>10,000	93.4 ± 10.4
19	N	(*S*)-PhCH(CH_3)	COCOHMe	6.0 ± 0.9	556 ± 67	15.4 ± 1.1

Table 2. SAR of aminopyridazines

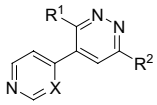

Compd	X	R^1	R^2	p38 (K_i, nM)	JNK3 (K_i, nM)	THP–TNF (IC_{50}, nM)
32	N	*m*CF_3-Ph	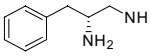	56.2 ± 2.8	>10,000	40.2 ± 3.8
33	N	*m*CF_3-Ph	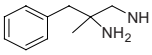	179.3 ± 4.2	>10,000	251.2 ± 7.4
34	C	Napht	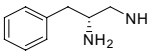	7.0 ± 0.5	735 ± 22	50.1 ± 6.3
35	C	Napht	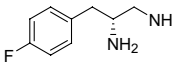	1.8 (n = 1)	1056 (n = 1)	92.2 (n = 1)
36	C	Napht	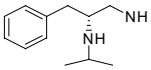	20.4 ± 0.3	598 ± 55	110 ± 17
37	C	Napht	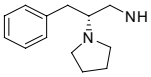	9.2 ± 0.2	81.5 ± 7.9	5.5 ± 0.3
38	C	Napht	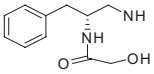	65.9 ± 5.2	211 ± 31	661 ± 93
39	C	Napht	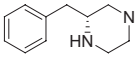	7.3 ± 0.2	160 ± 15	67.6 ± 3.0
40	C	Napht	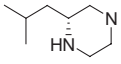	29.7 ± 1.9	650 ± 29	63.6 ± 6.4
41	C	Napht	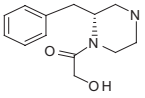	31.8 ± 0.6	72.5 ± 0.7	552.3 ± 51.8

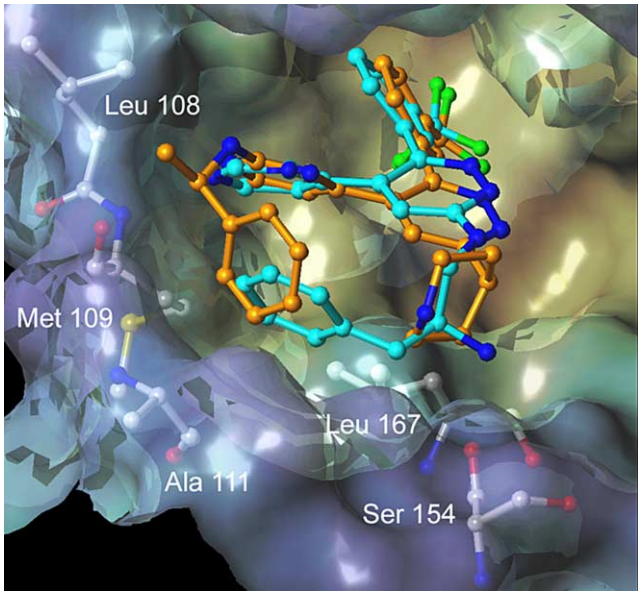

Figure 1. Model of **17** and **32** bound in the ATP-binding site of p38 MAP kinase.

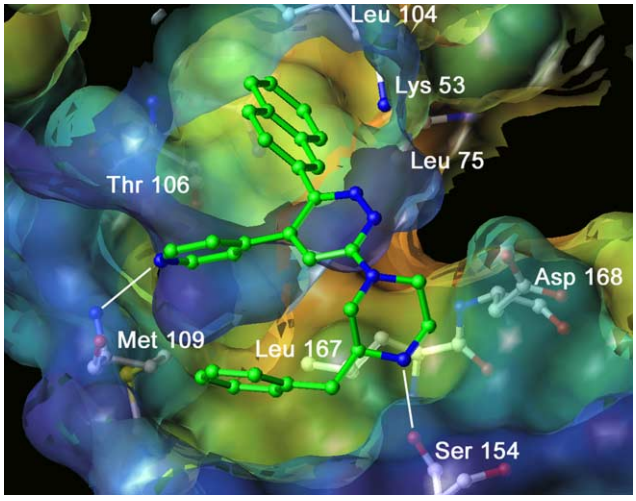

Figure 2. X-ray crystal structure of **39** cocrystallized with p38 MAP kinase.

36 and **37**); however, we observed a significant diminishing in cell potency (THP-1) and selectivity when the

Table 3. Inhibition of LPS induced TNF-α and IL-1β in human whole blood

Compd	WB TNF-α (IC_{50}, nM)	WB IL-1β (IC_{50}, nM)
10	5850 ± 8111	453 ± 513
17	1563 ± 738	610 ± 243
32	1827 ± 1667	2420 ± 2369
34	165 ± 34	454 ± 149
35	948 ± 28	974 ± 25
39	240 ± 57	415 ± 132
40	547 ± 331	550 ± 379

side chain nitrogen is acylated (**38** and **41**). We observed a good correlation between the binding and cell potency (THP-1) for most of these analogues.

To select compounds for further in vivo evaluation, we measured the activity of the most potent analogues in inhibiting the LPS-induced release of IL-1β and TNF-α from human whole blood (Table 3). This shift of potency in this assay relative to the p38 kinase inhibition assay provides information on the cell permeability and protein binding.[19]

Based on its potency and pharmacokinetic profile,[20] the pyridazine **39** was evaluated on two models of rheumatoid arthritis. In the murine LPS challenge model,[21] **39** has an ED_{50} of 1.28 mg/kg when administered orally 1 h prior to LPS challenge.

Compound **39** was also effective in the rat collagen induced arthritis (CIA) model,[22] when administered at 0.3, 1, and 3 mg/kg once a day beginning on day 11 through day 13. Pyridazine **39** inhibited paw swelling in this model dose dependently with an ED_{50} of 2.7 mg/kg.

In summary, two series of trisubstituted pyridazines have been identified as p38 inhibitors. Using molecular modeling and XR crystallography we were able to determine that the two different classes occupied a similar space in the protein binding pocket. Pyridazine **39** from this series showed oral efficacy in the mouse LPS and rat CIA in vivo models. Additional SAR studies directed toward increasing potency in the cell-based assays would be required before any compound from this class could be advanced further.

References and notes

1. Foster, M. L.; Halley, F.; Souness, J. E. *Drug News Perspect.* **2000**, *13*, 488.
2. Rutgeerts, P.; D'Haens, G.; Targan, S.; Vasiliauskas, E.; Hanauer, S. B.; Present, D. H.; Mayer, L.; Van Hogezand, R. A.; Braakman, T.; DeWoody, K. L.; Schaible, T. F.; Van Deventer, S. J. H. *Gastroenterology* **1999**, *117*, 761.
3. Paul, A.; Wilson, S.; Belham, C. M.; Robinsson, C. J. M.; Scott, P. H.; Gould, G. W.; Plevin, R. *Cell. Signalling* **1997**, *9*, 403.
4. Han, J.; Lee, J. D.; Jiang, Y.; Li, Z.; Feng, L.; Ulevitch, R. J. *J. Biol. Chem.* **1996**, *271*, 2886.
5. Raingeaud, J.; Gupta, S.; Rogers, J. S.; Dickens, M.; Han, J.; Ulevitch, R. J.; David, R. J. *J. Biol. Chem.* **1995**, *270*, 7420.
6. McIntyre, C. J.; Ponticello, G. S.; Liverton, N. J.; O'Keefe, S. J.; O'Neill, E. A.; Pang, M.; Schwartz, C. D.; Claremon, D. A. *Bioorg. Med. Chem. Lett.* **2002**, *12*, 689.
7. Tisler, M.; Stanovnik, B. In *Comprehensive Heterocyclic Chemistry*; Katritzky, A. R., Rees, C. W., Eds.; Pergamon: Oxford, 1984; Vol. 3, p 45.
8. Strekowski, L.; Wydra, R. L.; Janda, L.; Harden, D. B. *J. Org. Chem.* **1991**, *56*, 5610.
9. De Lazlo, S. E.; Mantlo, N. B.; Ponticello, G. S.; Selnick, H. G.; Liverton, N. J. WO9705877A1; *Chem. Abstr*. **1997**, *126*, 225212.
10. Blacklock, T. J.; Sohar, P.; Butcher, J. W.; Lamanec, T.; Grabowski, E. J. *J. Org. Chem.* **1993**, *58*, 1672.
11. For a review see: Boehm, J. C.; Adams, J. L. *Expert Opin. Ther. Pat.* **2000**, *10*, 25.
12. Lee, J. C.; Kassis, S.; Kumar, S.; Badger, A.; Adams, J. L. *Pharmacol. Ther.* **1999**, *82*, 389.
13. Adams, J. L.; Boehm, J. C.; Kassis, S.; Gorycki, P. D.; Webb, E. F.; Hall, R.; Sorenson, M.; Lee, J. C.; Ayrton, A.; Griswold, D. E.; Gallagher, T. F. *Bioorg. Med. Chem. Lett.* **1998**, *8*, 3111.
14. (a) McLay, I. M.; Halley, F.; Souness, J. E.; McKenna, J.; Benning, V.; Birrell, M.; Burton, B.; Belvisi, M.; Collis, A.; Constan, A.; Foster, M.; Hele, D.; Jayyosi, Z.; Kelley, M.; Maslen, C.; Miller, G.; Ouldelhkim, M.-C.; Page, K.; Phipps, S.; Pollock, K.; Porter, B.; Ratcliffe, A. J.; Redford, E. J.; Webber, S.; Slater, B.; Thybaud, V.; Wilsher, N. *Bioorg. Med. Chem.* **2001**, *9*, 537; (b) Liverton, N. J.; Butcher, J. W.; Claiborne, C. F.; Claremon, D. A.; Libby, B. E.; Nguyen, K. T.; Pitzenberger, S. M.; Selnick, H. G.; Smith, G. R.; Tebben, A.; Vacca, J. P.; Varga, S. L.; Agarwal, L.; Dancheck, K.; Forsyth, D. S.; Fletcher, D. S.; Frantz, B.; Hanlon, W. A.; Harper, C. F.; Hofsess, S. J.; Kostura, M.; Lin, J.; Luell, S.; O'Neil, E. A.; Orevillo, C. J.; Pang, M.; Parsons, J.; Rolando, A.; Sahly, Y.; Visco, D. M.; O'Keefe, S. J. *J. Med. Chem.* **1999**, *42*, 2180.
15. Park, Y. W.; Cummings, R. T.; Wu, L.; Zheng, S.; Cameron, P. M.; Woods, A.; Zaller, D. M.; Marcy, A. I.; Hermes, J. D. *Anal. Biochem.* **1999**, *269*, 94.
16. Whole cell potency in LPS treated THP-1 cells was determined by measuring secreted TNF-α using an electrochemiluminescence immunoassay.
17. Unpublished data.
18. Refined crystallographic coordinates for the structure of p38α complexed with **39** have been deposited with the Protein Data Bank (http://www.rscb.org) with entry code 1YQJ.
19. There seemed to be no clear explanation for the discrepancy between inhibition of p38α and whole blood potency in these series. These compounds have very similar physicochemical characteristics.
20. Pharmacokinetic properties of compound **39** in rat (bioavailability: 30%; $t_{1/2}$: 2.2 h; C_{max}: 0.13 μM @ 10 mg/kg po). Pyridinylpyridazine **39** was devoid of human p450 inhibition. [Isoenzyme: IC_{50} (μM); CYP2D6 > 30; CYP3A4 > 30].
21. Vehicle or compound was administered po to BALB/c mice ($n = 5$) 1 h before giving LPS (10 mg/mice, iv). Blood was collected 90 min later and serum TNF-α levels were determined using a Biosource ELISA kit. % Inhibition of TNF-α production was calculated using the formula [(vehicle control − compound)/(vehicle control)] × 100.
22. Trentham, D. E.; Townes, A. S.; Kang, A. H. *J. Exp. Med.* **1977**, *146*, 857.